

SUPPLEMENTARY MATERIAL

Effects of a mixture of ligands on metal accumulation in diffusive gradients in thin films (DGT)

Alexandra Altier,^A Martín Jiménez-Piedrahíta,^A Ramiro Uribe,^B Carlos Rey-Castro,^A Joan Cecília,^C Josep Galceran^A and Jaume Puy^{A,D}

^ADepartament de Química, Universitat de Lleida, and Agrotecnio, Rovira Roure 191, 25198 Lleida, Catalonia, Spain.

^BDepartment of Physics, University of Tolima, 730006 Ibagué, Colombia.

^CDepartament de Matemàtica, Universitat de Lleida, and Agrotecnio, Rovira Roure 191, 25198 Lleida, Catalonia, Spain.

^DCorresponding author. Email: jpuy@quimica.udl.cat

Table of Contents

1. Experimental systems	2
1.1 DGT deployment procedure	6
1.2 DGT accumulations	7
2. General Mathematical Formulation.....	10
3. Fitting the experimental accumulations.....	11
4. Formulation of the NiNTA and NiEN systems in terms of only one complex species.....	14
4.1 The case of NiNTA.....	17
4.2 The case of NiEN.....	18
5. Dependence of the lability degree on the ligand concentration in a single ligand system.....	19
6. Dependence of the metal accumulation on the stoichiometry of MEN complex ...	20

1. Experimental systems

Experiments at nominal elemental concentrations reported in Table 1 of the main text for Ni, NTA and EN in separate or mixed systems were done at pH 8 and salt background $50 \text{ mol}\cdot\text{m}^{-3}$. Current concentrations in the bulk solution were determined with ICP-MS measurements. Values are reported in Table S1

Table S1. Ni concentrations measured in the bulk solution of the single ligand experiments and in the mixture with ICP-MS.

Parameters	Single ligand systems (mol m^{-3})		Mixed ligand system (mol m^{-3})
	Ni + NTA	Ni + EN	
$C_{\text{T,Ni}}^*$	9.2×10^{-3}	2.4×10^{-2}	2.3×10^{-2}
$C_{\text{T,NTA}}^*$	10^{-2}	-	10^{-2}
$C_{\text{T,EN}}^*$	-	1	1
HEPES	1	1	1
I	50	50	50
pH	8.01 ± 0.01	8.00 ± 0.01	8.02 ± 0.02
T (°C)	25.0 ± 0.1	25.0 ± 0.1	25.0 ± 0.1

Once these concentrations are used as input values in Visual MINTEQ, speciation results reported in Tables S2 and S3 are obtained.

Table S2. Percentage of the species formed in single and mixed ligand system under experimental conditions specified in Table S1.

Component	% of total concentration			Species name
	Single ligand system NiNTA	Single ligand system NiEN	Mixed ligand system	
Ni ²⁺	0.016	0.041	0.022	Ni ²⁺
	-	6.893	3.881	NiEN
	-	84.454	48.634	Ni(EN) ₂
	-	8.607	5.069	Ni(EN) ₃
	99.84	-	42.344	NiNTA ⁻
	0.051	-	-	Ni(NTA) ₂ ⁴⁻
	0.09	-	0.038	NiOHNTA ²⁻
EN	-	0.8	0.818	EN
NTA ³⁻	0.106	-	0.033	NTA ³⁻

Table S3. Speciation in SLS and in the mixture under the experimental conditions specified in Table S1, using the speciation program Visual MINTEQ.

Species name	SLS NiNTA (mol m ⁻³)	SLS NiEN (mol m ⁻³)	Mixture (mol m ⁻³)
CO ₃ ²⁻	5.94×10 ⁻³	5.96×10 ⁻³	5.96×10 ⁻³
EN	-	8.00×10 ⁻³	8.18×10 ⁻³
HEN	-	8.37×10 ⁻¹	8.56×10 ⁻¹
H ⁺	1.22×10 ⁻⁵	1.22×10 ⁻⁵	1.22×10 ⁻⁵
H ₂ EN	-	1.07×10 ⁻¹	1.09×10 ⁻¹
H ₂ CO ₃ [*] (aq)	1.28×10 ⁻²	1.28×10 ⁻²	1.28×10 ⁻²
H ₂ NTA ⁻	3.88×10 ⁻⁹	-	1.18×10 ⁻⁹
H ₃ NTA (aq)	3.15×10 ⁻¹⁵	-	9.54×10 ⁻¹⁶
H ₄ NTA ⁺	3.88×10 ⁻²²	-	1.18×10 ⁻²²
HCO ³⁻	7.00×10 ⁻¹	7.00×10 ⁻¹	7.00×10 ⁻¹
HEPES ⁻	7.71×10 ⁻¹	7.71×10 ⁻¹	7.71×10 ⁻¹
H-HEPES (aq)	2.29×10 ⁻¹	2.29×10 ⁻¹	2.29×10 ⁻¹
HNTA ²⁻	7.95×10 ⁻⁴	-	2.42×10 ⁻⁴

Na⁺	$4.95 \times 10^{+1}$	$4.95 \times 10^{+1}$	$4.95 \times 10^{+1}$
NaCO³⁻	2.48×10^{-3}	2.48×10^{-3}	2.48×10^{-3}
NaHCO₃ (aq)	1.16×10^{-2}	1.15×10^{-2}	1.15×10^{-2}
NaNO₃ (aq)	4.60×10^{-1}	4.59×10^{-1}	4.60×10^{-1}
NaNTA²⁻	1.14×10^{-5}	-	3.45×10^{-6}
NaOH (aq)	5.08×10^{-5}	5.08×10^{-5}	5.08×10^{-5}
Ni(NTA)₂⁴⁻	4.82×10^{-6}	-	1.58×10^{-6}
Ni(OH)₂ (aq)	6.65×10^{-10}	4.41×10^{-9}	2.33×10^{-9}
Ni(OH)₃⁻	8.24×10^{-13}	5.47×10^{-12}	2.89×10^{-12}
NiEN	-	1.65×10^{-3}	8.93×10^{-4}
Ni(EN)₂	-	2.03×10^{-2}	1.12×10^{-2}
Ni(EN)₃	-	2.07×10^{-3}	1.17×10^{-3}
Ni⁺²	1.47×10^{-6}	9.78×10^{-6}	5.16×10^{-6}
NiCO₃ (aq)	6.59×10^{-8}	4.37×10^{-7}	2.30×10^{-7}
NiHCO³⁺	5.75×10^{-8}	3.82×10^{-7}	2.01×10^{-7}
NiNO³⁺	8.29×10^{-8}	5.50×10^{-7}	2.90×10^{-7}
NiNTA⁻	9.17×10^{-3}	-	9.74×10^{-3}
NiOH⁺	1.03×10^{-8}	6.82×10^{-8}	3.60×10^{-8}
NiOHNTA²⁻	8.30×10^{-6}	-	8.84×10^{-6}
NO₃⁻	$4.95 \times 10^{+1}$	$4.96 \times 10^{+1}$	$4.96 \times 10^{+1}$
NTA³⁻	1.09×10^{-5}	-	3.32×10^{-6}
OH⁻	1.22×10^{-3}	1.23×10^{-3}	1.23×10^{-3}
NTA^{eff}	8.17×10^{-4}	-	2.49×10^{-4}
EN^{eff}	-	9.52×10^{-1}	9.73×10^{-1}

Total concentrations were chosen to reach, in equilibrium, a negligible free metal concentration and to ensure that the accumulation is only due to the complex contribution. The effects of the mixture on the lability degree are then expected to be more noticeable. Moreover, pH 8 was selected since it leads to a free Ni concentration in the mixed system smaller than 1% of the total Ni concentration (See Table S1). A free Ni concentration corresponding to 3.9 % of the total is, for instance, predicted at pH 7.

The lability degree of a given complex species changes in the presence of a mixture of ligands¹. The change is more evident for partially labile complexes which can vary on both directions (increasing or decreasing lability)². We have, then, included a partially labile complex in the mixture. Indeed, at ionic strength 50 mol m^{-3} , the complex NiNTA shows a partially labile behaviour³ and the complex NiEN has a labile behaviour⁴.

Concentrations of the different solutions have been selected to keep common bulk concentrations of free metal, complex and free ligand in the mixture and in the corresponding SLS. We aim at using $\xi_i^{h=1}$ values as surrogates of ξ_i in the mixture and assessing the accuracy of this estimation of the metal accumulation in the mixtures. As seen in Table S3, due to the experimental random errors, total concentrations used in the SLS do not lead to common bulk concentrations of free metal, complex and ligand than in the mixture. For instance, the NTA^{eff} concentration in the SLS is close to three times the concentrations that it has in the mixture. An important part of this difference comes from the small change between the nominal concentrations indicated in Table 1 of the main text and those in the bulk solution measured by ICP-MS (Table S1) as can be confirmed with the speciation prediction of VMINTEQ.

According to the values in Table S3, neglecting the ionic pairs, the desired values of total Ni and total NTA in the SLS are 9.745×10^{-3} and $9.989 \times 10^{-3} \text{ mol} \cdot \text{m}^{-3}$, respectively instead of those found in Table S1. These small differences do not modify $\xi_{\text{NiNTA}}^{h=1}$, since the condition $c_{\text{T,NTA}}^* > 0.625 c_{\text{T,Ni}}^*$ (indicated in Section 3.1.1 of the main text as a rough estimation of the minimum $c_{\text{T,NTA}}^*$ that ensures that the lability degree of the NiNTA is that of the excess of ligand conditions) is fulfilled by both the actual SLS concentrations reported in Table S1 and those reported in this paragraph.

For the NiEN system, the differences between the free EN^{eff} concentration in the SLS and in the mixture increase. However, no effects are expected from this change, since EN^{eff} is in excess of ligand conditions where the lability degree has been shown to be almost independent of the ligand concentration.

1.1 DGT deployment procedure

DGT pistons and cap mouldings were cleaned overnight where the following sequence was always assumed: they were soaked in 2% phosphate-free, surface-active detergent called DECON-90 supplied by Decon Laboratories Limited, Sussex, U.K. Afterwards, they remained in Milli-Q water at least one day. At that point, they were washed with Milli-Q water until bubbles disappeared.⁵ Then, they were cleaned using four 1 h 10% nitric acid (Analytical Reagent Grade, Fisher Chemical) soaks. Finally, they were rinsed with Milli-Q water until the pH is around 5.

Prior to the serial-time deployments, the assembled DGT samples were immersed for at least 18 hours in a pre-conditioning solution with the same pH and ionic strength as the test solution.

A 5 L polyethylene container, pre-cleaned by using three 24 h 10% HNO_3 soaks, was thermostated at 25.0 ± 0.1 °C controlled by a thermostatic bath where the test solution container was introduced and was stirred at 240 rpm using an overhead stirrer. To provide a well-stirred solution (to ensure that the diffusive boundary layer, DBL, thickness is negligible compared with the total thickness summation of the filter and diffusive gel thickness⁶⁻⁸), the solution was stirred continuously. Prior to deploying the DGT samplers in 2 L of test solution, the solution was stirring for at least 24 hours to equilibrate and the pH was adjusted to the desired value by adding diluted HNO_3 or NaOH as explained above. pH was measured during the deployment of the DGT sensors using a pH meter Orion 920A+ (Thermo Electron Corporation). Ultrapure water

with resistivity $\geq 18 \mu\Omega \text{ cm}$ (Synergy UV purification system Millipore) was used in all preparations. Three sets of triplicate DGT sensors were deployed in the solutions and retrieved after 8, 16 and 24 hours. 1 mL aliquots of the test solution were taken at regular intervals of time to control the total amount of metal. After deployment, the DGT samples were retrieved and then rinsed with Milli-Q water, the fitted cap was removed, and the resin layers were carefully placed into 1.5 mL micro-centrifuge PVC tubes. Metals were eluted from retrieved membranes by immersing them in 1 mL of 20% HNO_3 (TraceMetal Grade, Fisher Chemical) for at least 24 hours to allow an efficient metal extraction from the resin.

Samples were diluted 50-fold and deployment solutions and metal accumulations were analyzed by inductively coupled plasma mass spectrometry (ICP-MS, 7700 Series, Agilent).

The mass of the metal accumulated in the resin was calculated as,

$$n = c_e(V_e + V_g) / f_e \quad (\text{S1})$$

where n is the amount of metal accumulated in the resin, c_e is the concentration from ICP-MS measurements of the eluted resin gel (mol m^{-3}), V_e is the eluent volume, V_g is the resin gel volume and f_e is the elution factor, in this case 1⁹.

1.2 DGT accumulations

Accumulation results are shown in Figure S1 and S2 for SLS and Figure S3 for the mixture.

Table S4. Total experimental accumulation of Ni and back percentage for different deployment times for SLS and mixed ligand system.

	SLS NiNTA		SLS NiEN		Mixed ligand system	
Time (h)	n_T (nmol)	%back	n_T (nmol)	%back	n_T (nmol)	%back
8	23	40	117	5	72	13
16	40	41	244	7	138	15
24	63	47	362	4	224	12

The accumulated mass of Ni in devices with two resin layers, labelled front (F) and back (B), was converted to concentration by using Eqn. (S1) and values of diffusion coefficients reported in the main text. Values are expressed as ratios of amount of metal (nmol) over bulk concentration to refer the measurement to a fixed metal concentration avoiding dilution effects.

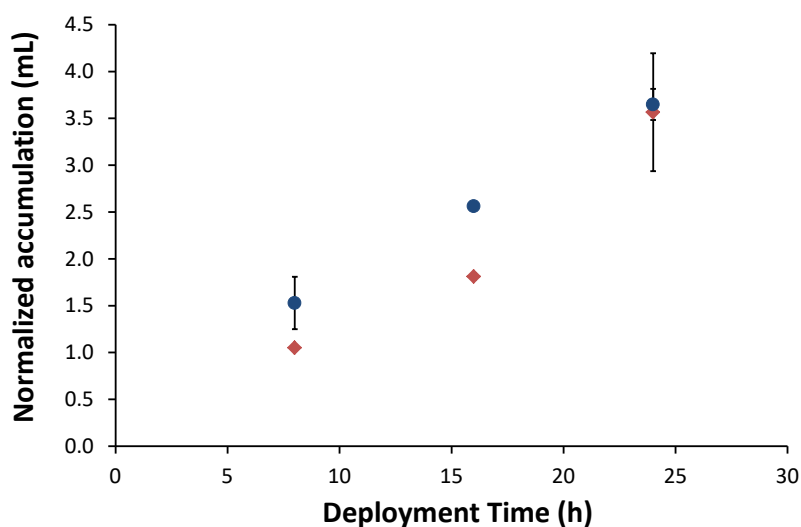


Figure S1. Time-series of DGT normalized accumulation (nmol/c^*) in a SLS NiNTA in the front (red bullet) and in the back (blue diamond) at 25 °C. Experimental conditions as mentioned in Table S1. Error bars refer to standard deviations.

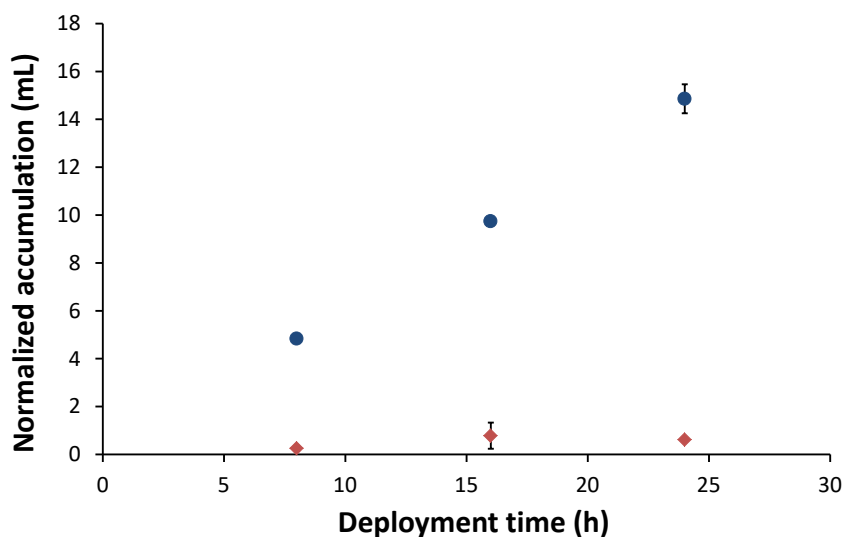


Figure S2. Time-series of DGT normalized accumulation (nmol/c^*) in a SLS NiEN in the front (red bullet) and in the back (blue diamond) at 25 °C. Experimental conditions as mentioned in Table S1. Error bars refer to standard deviations.

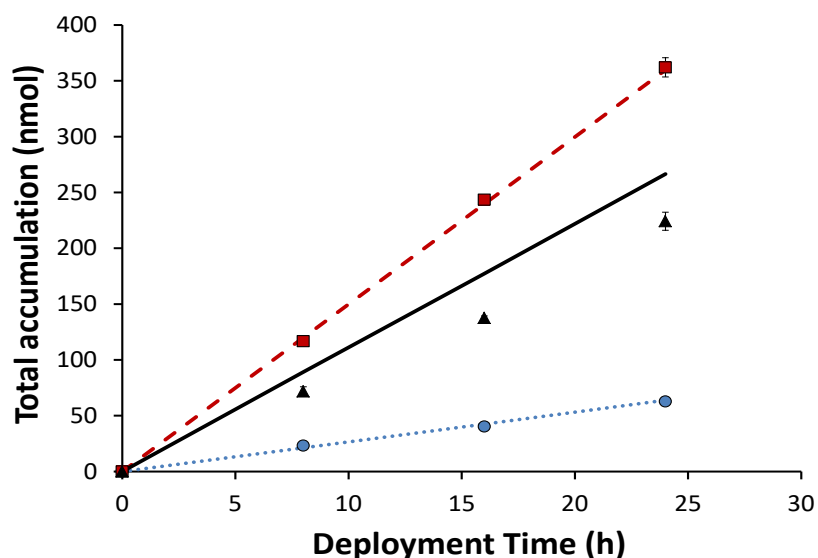


Figure S3. Time evolution of the total accumulation of Ni in DGT devices with two resin discs. Markers correspond to experimental accumulations of Ni in SLS NiNTA (blue circle), SLS NiEN (red square) and in the mixed ligand system (black triangle). Dashed line corresponds to Ni accumulation assuming perfect-sink conditions for SLS NiEN. Dotted line corresponds to Ni accumulation assuming perfect-sink conditions for SLS NiNTA. Continuous line corresponds to the Ni accumulation using the values obtained from Eq. 28 in the main text. Experimental conditions as mentioned in Table S1 for each experiment. Error bars refer to standard deviations.

Table S5 . Normalized accumulation of Ni (accumulated moles over the bulk concentration) in DGT devices with two resin gels after 8, 16 and 24 h deployment normalized by bulk solutions in single ligand systems. Experimental conditions are reported in Table S1.

Time (h)	sensor	$n_{\text{Ni}}^{\text{only NTA}} / c_{\text{T,Ni}}^*$ (mL)	$n_{\text{Ni}}^{\text{only EN}} / c_{\text{T,Ni}}^*$ (mL)
8	F	1.53 ± 0.28	4.84 ± 0.14
	B	1.05 ± 0.01	0.25 ± 0.10
	% Back	39.77 ± 4.77	4.90 ± 1.76
16	F	2.56 ± 0.03	9.74 ± 0.18
	B	1.81 ± 0.03	0.78 ± 0.55
	% Back	40.79 ± 0.70	7.31 ± 4.95
24	F	3.65 ± 0.17	14.86 ± 0.61
	B	3.57 ± 0.63	0.61 ± 0.03
	% Back	46.97 ± 4.23	3.91 ± 0.30

2. General Mathematical Formulation

For the range of concentrations used in this work, the relevant complexation reactions of Ni with NTA are:



and the relevant complexation reactions of Ni with EN are:



Additionally, the reaction of Ni with the Chelex beads in the resin domain has also to be considered:



Full mathematical formulation for the SLS or the mixture has been done by writing the pertaining reaction-diffusion equations. Boundary conditions include bulk concentrations at the diffusive gel/bulk solution interface and flux null at the bottom of the resin domain corresponding to $x=0$. Continuity of the flux of each species has been considered at the resin diffusive gel interface. Numerical solution of the resulting system can be achieved with the simulation tool especially written to analyse mixture systems and described in the SI of ^{10,11}. Finite Element Method is used for the solution of the spatial dependence, while Finite Differences are used for the temporal dependence.

In order to include in the simulation the effect of the buffer to keep pH constant, reaction-diffusion equations for a buffer (HA) have also been considered. Thus additional species, HA, A and H have been introduced at concentrations high enough to keep pH constant and equal to the desired value (bulk concentrations of HA, A and H are 81.7, 18.3 and 10^{-5} mol m⁻³, respectively).

3. Fitting the experimental accumulations

For the simulations, it was assumed that the diffusion coefficients of ligands, protonated ligands and complexes are equal. The value of the diffusion coefficient of Ni was taken from ¹². For species involved in the buffer reaction (H, A, HA), the value for the diffusion coefficient was assumed very high, in comparison with the values for other species, to have an homogeneous pH value. Values for these coefficients are presented in Table S6.

Table S6. Diffusion coefficients of species used in simulations

Species	D ($\text{m}^2 \text{s}^{-1}$)
Ni	6.08×10^{-10}
NTA, NiNTA, HNTA	4.75×10^{-10}
EN, NiEN, Ni(EN) ₂ , Ni(EN) ₃ , HEN, H ₂ EN	6.08×10^{-10}
H, A, HA	1.00×10^{-8}

Migration effects were considered using the partition model explained in ¹⁰. The Boltzmann factor was measured experimentally as explained in the main manuscript. For $I=0.051 \text{ mol L}^{-1}$, a value of $\Pi = 2.0$ was used in simulations.

Stability constants for reactions (S2) - (S8) were obtained from Visual MINTEQ 3.1.

Assuming that the formation/dissociation of NiEN is the rate limiting step in the stepwise complexation, the kinetic rate constants for the formation/dissociation of Ni(EN)₂ and Ni(EN)₃ were selected high enough to neglect their influence in the results, but keeping the ratio $k_{a,\text{Ni(EN)}_i} / k_{d,\text{Ni(EN)}_i}$ equal to the equilibrium constant $K_{\text{Ni(EN)}_i}$.

Additionally, all the protonation reactions are assumed to be fast enough to reach equilibrium instantaneously, so that the acid base equilibrium relationships apply.

Appropriate values for the kinetic constants ($k_{a,\text{NiNTA}}$ and $k_{d,\text{NiNTA}}$) were selected to fit the Ni accumulations for the single NiNTA system presented in Table S8. Experimental and calculated accumulations for the fitted values of the kinetic constants are reported in Table S8a.

The system NiEN is almost fully labile. Accordingly, the accumulation is almost independent of the particular kinetic constant $k_{d,\text{NiEN}}$ and the lowest value approaching the accumulation within a 2% discrepancy was selected. Additionally, the stability

constant reported in Visual MINTEQ was used. Experimental and calculated accumulations for the fitted values of the kinetic constants are reported in Table S8b.

The kinetic and the stability constants for the reaction of Ni with the resin sites appearing in Eqn. (S9) were assumed high enough to simulate perfect sink conditions.

The set of parameters used in the complexation reactions NiNTA, NiEN and NiR are gathered in Table S7.

Table S7. Kinetic and stability constants for reactions used in simulations for systems with Ni, NTA and EN.

Reaction	k_a ($\text{m}^3\text{mol}^{-1}\text{s}^{-1}$)	k_d (s^{-1})	K ($\text{m}^3\text{mol}^{-1}$)
$\text{Ni} + \text{NTA} \xrightleftharpoons[k_{d,\text{NiNTA}}]{k_{a,\text{NiNTA}}} \text{NiNTA}$	1.90×10^6	3.32×10^{-3}	5.72×10^8
$\text{H} + \text{NTA} \xrightleftharpoons[k_{d,\text{HNTA}}]{k_{a,\text{HNTA}}} \text{HNTA}$	7.29×10^6	1.00	7.29×10^6
$\text{Ni} + \text{EN} \xrightleftharpoons[k_{d,\text{NiEN}}]{k_{a,\text{NiEN}}} \text{NiEN}$	1.00×10^6	46.9	2.13×10^4
$\text{NiEN} + \text{EN} \xrightleftharpoons[k_{d,\text{Ni}(\text{EN})_2}]{k_{a,\text{Ni}(\text{EN})_2}} \text{Ni}(\text{EN})_2$	1.53×10^3	1.00	1.53×10^3
$\text{Ni}(\text{EN})_2 + \text{EN} \xrightleftharpoons[k_{d,\text{Ni}(\text{EN})_3}]{k_{a,\text{Ni}(\text{EN})_3}} \text{Ni}(\text{EN})_3$	12.7	1.00	12.74
$\text{H} + \text{EN} \xrightleftharpoons[k_{d,\text{HEN}}]{k_{a,\text{HEN}}} \text{HEN}$	1.05×10^7	1.00	1.05×10^7
$\text{H} + \text{HEN} \xrightleftharpoons[k_{d,\text{H}_2\text{EN}}]{k_{a,\text{H}_2\text{EN}}} \text{H}_2\text{EN}$	1.28×10^4	1.00	1.28×10^4
$\text{H} + \text{A} \xrightleftharpoons[k_{d,\text{HA}}]{k_{a,\text{HA}}} \text{HA}$	4.47×10^5	1.00	4.47×10^5
$\text{Ni} + \text{R} \xrightleftharpoons[k_{d,\text{NiR}}]{k_{a,\text{NiR}}} \text{NiR}$	10^{15}	1.00	10^{15}

Table S8. Total accumulation of Ni and back percentage for different deployment times for panel a) SLS NiNTA and panel b) SLS NiEN obtained experimentally and by simulation.

a)

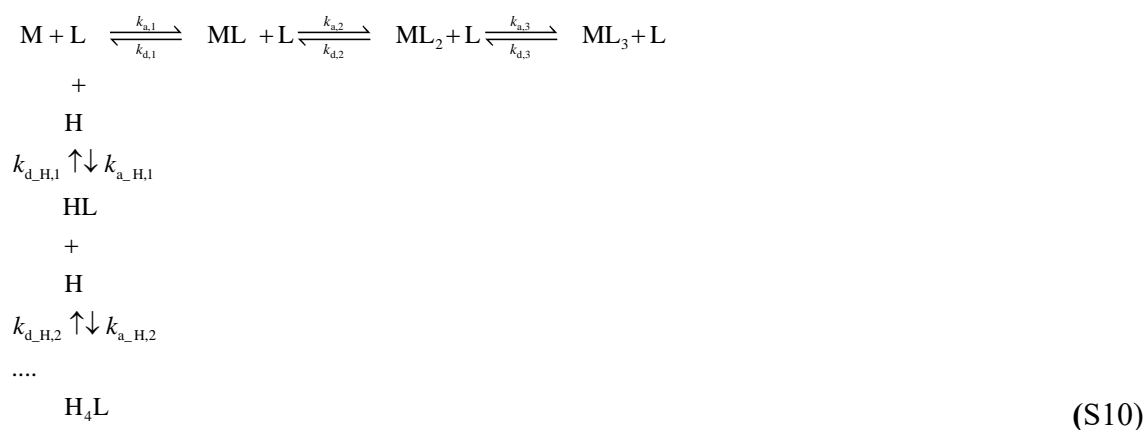
SLS NiNTA				
Time (h)	$n_{T,exp}$ (nmol)	%back _{,exp}	$n_{T,calc}$ (nmol)	%back _{,calc}
8	23	40	21	30
16	40	41	42	30
24	63	47	62	30

b)

SLS NiEN				
Time (h)	$n_{T,exp}$ (nmol)	%back _{,exp}	$n_{T,calc}$ (nmol)	%back _{,calc}
8	117	5	119	0
16	244	7	238	0
24	362	4	357	0

4. Formulation of the NiNTA and NiEN systems in terms of only one complex species.

A general scheme of the volume reactions in the systems NiNTA and NiEN is:



where M stands for Ni while L stands for either NTA or EN. $k_{a,j}$ and $k_{d,j}$ label the association and dissociation rate constants, respectively.

Eqn. (S10) indicates that the metal can form different complex species of different M:L stoichiometric ratios which is the case of the reaction of Ni with EN, while L is also involved in acid-base equilibria, which applies to both NTA and EN.

We assume that i) the formation/dissociation of ML is the rate limiting step in the stepwise complexation of the metal M with the ligand L so that ML_2 and ML_3 can be instantaneously related to ML through the equilibrium relationships and ii) all the protonation reactions are fast enough to reach equilibrium instantaneously so that the acid base equilibrium relationships apply:

$$K_{H,i} = \frac{c_{H_i L}}{c_H^i c_{H_{(i-1)} L}} \quad (S11)$$

Under these conditions, defining the bound metal, c_{M_b} , as:

$$c_{M_b} = c_{ML} + c_{ML_2} + c_{ML_3} \quad (S12)$$

and c_L^{eff} as an effective concentration of ligand corresponding to all the ligand species without metal bound,

$$c_L^{\text{eff}} = c_L + c_{HL} + c_{H_2L} + c_{H_3L} + c_{H_4L} \quad (S13)$$

a closed system of differential reaction-diffusion equations for c_M , c_{M_b} and c_L^{eff} can be written as¹³:

$$\frac{\partial c_M}{\partial t} = D_M \frac{\partial^2 c_M}{\partial x^2} + \frac{k_{d,1}}{1 + \frac{K_2 c_L^{\text{eff}}}{B} + \frac{K_2 K_3 (c_L^{\text{eff}})^2}{B^2}} c_{M_b} - \frac{k_{a,1}}{B} c_M c_L^{\text{eff}} \quad (S14)$$

$$\frac{\partial c_{M_b}}{\partial t} = \left(\frac{D_{ML} + D_{ML_2} \frac{K_2 c_L^{\text{eff}}}{B}}{1 + \frac{K_2 c_L^{\text{eff}}}{B} + \frac{K_2 K_3 (c_L^{\text{eff}})^2}{B^2}} \right) \frac{\partial^2 c_{M_b}}{\partial x^2} - \frac{k_{d,1}}{1 + \frac{K_2 c_L^{\text{eff}}}{B} + \frac{K_2 K_3 (c_L^{\text{eff}})^2}{B^2}} c_{M_b} + \frac{k_{a,1}}{B} c_M c_L^{\text{eff}} \quad (S15)$$

and

$$\frac{\partial c_L^{\text{eff}}}{\partial t} = D_L \frac{\partial^2 c_L^{\text{eff}}}{\partial x^2} + \frac{k_{d,1}}{1 + \frac{K_2 c_L^{\text{eff}}}{B} + \frac{K_2 K_3 (c_L^{\text{eff}})^2}{B^2}} c_{M_b} - \frac{k_{a,1}}{B} c_M c_L^{\text{eff}} \quad (\text{S16})$$

where D_i stands for the diffusion coefficient of species i ,

$$B = 1 + K_{H,1} c_H + K_{H,1} K_{H,2} c_H^2 + K_{H,1} K_{H,2} K_{H,3} c_H^3 + K_{H,1} K_{H,2} K_{H,3} K_{H,4} c_H^4 \quad (\text{S17})$$

$$K_i = \frac{k_{a,i}}{k_{d,i}} \quad (\text{S18})$$

and $K_{H,i}$ stand for the association acid constants as indicated in Eqn. (S11).

Equations (S12) to (S16) are formally identical to a system with one ligand with concentration c_L^{eff} , that is not involved in any protonation and formation of multiple equilibria with the metal, whenever the system is in excess of ligand conditions and a buffer or a fast enough diffusion of the protons ensures a homogenous concentration profile for c_H . Indeed, only under these conditions the effective association and dissociation constants of this metal to ligand effective reaction are constant and given by:

$$k_a^{\text{eff}} = \frac{k_{a,1}}{B} \quad (\text{S19})$$

$$k_d^{\text{eff}} = \frac{k_{d,1}}{1 + \frac{K_2 c_L^{\text{eff}}}{B} + \frac{K_2 K_3 (c_L^{\text{eff}})^2}{B^2}} \quad (\text{S20})$$

The effective stability constant of the metal complexation with this formal ligand c_L^{eff} is:

$$K^{\text{eff}} = \frac{k_a^{\text{eff}}}{k_d^{\text{eff}}} = \frac{K_1 \left(1 + \frac{K_2 c_L^{\text{eff}}}{B} + \frac{K_2 K_3 (c_L^{\text{eff}})^2}{B^2} \right)}{B} \quad (\text{S21})$$

The effective diffusion coefficients of the effective species are given by:

$$D_{ML}^{\text{eff}} = \frac{D_{ML} + D_{ML_2} \frac{K_2 c_L^{\text{eff}}}{B} + D_{ML_3} \frac{K_2 c_L^{\text{eff}}}{B} \frac{K_3 c_L^{\text{eff}}}{B}}{1 + \frac{K_2 c_L^{\text{eff}}}{B} + \frac{K_2 c_L^{\text{eff}}}{B} \frac{K_3 c_L^{\text{eff}}}{B}} \quad (\text{S22})$$

and

$$D_L^{\text{eff}} = D_L \quad (\text{S23})$$

4.1 The case of NiNTA

Equations (S19)-(S22) for the NiNTA SLS become:

$$k_{a,\text{NiNTA}}^{\text{eff}} = \frac{k_{a,\text{NiNTA}}}{1 + K_{\text{HNTA}} c_H} \quad (\text{S24})$$

$$k_{d,\text{NiNTA}}^{\text{eff}} = k_{d,\text{NiNTA}} \quad (\text{S25})$$

$$K_{\text{NiNTA}}^{\text{eff}} = \frac{k_{a,\text{NiNTA}}^{\text{eff}}}{k_{d,\text{NiNTA}}^{\text{eff}}} = \frac{K_{\text{NiNTA}}}{1 + K_{\text{HNTA}} c_H} \quad (\text{S26})$$

$$c_{\text{NTA}}^{\text{eff}} = c_{\text{NTA}} + c_{\text{HNTA}} \quad (\text{S27})$$

and

$$D_{\text{NTA}}^{\text{eff}} = D_{\text{NTA}} \quad (\text{S28})$$

The use of these effective parameters allows to rewrite the processes described in Eqns.

(S2)-(S3) as only one process:



being $k_{a,\text{NiNTA}}^{\text{eff}}$ a real constant because H/OH diffuse faster than the rest of ions

diffusivity and we use a buffer to keep pH constant.

4.2 The case of NiEN

For the effective complexation process



Equations (S19)-(S22) become:

$$k_{\text{a,NiEN}}^{\text{eff}} = \frac{k_{\text{a,NiEN}}}{B} \quad (\text{S31})$$

$$k_{\text{d,NiEN}}^{\text{eff}} = \frac{k_{\text{d,NiEN}}}{1 + \frac{K_{\text{Ni(EN)}_2} c_{\text{EN}}^{\text{eff}}}{B}} \quad (\text{S32})$$

$$B = 1 + K_{\text{HEN}} c_{\text{H}} + K_{\text{HEN}} K_{\text{H}_2\text{EN}} c_{\text{H}}^2 \quad (\text{S33})$$

$$K_{\text{NiEN}}^{\text{eff}} = \frac{k_{\text{a,NiEN}}^{\text{eff}}}{k_{\text{d,NiEN}}^{\text{eff}}} \quad (\text{S34})$$

with:

$$c_{\text{EN}}^{\text{eff}} = c_{\text{EN}} + c_{\text{HEN}} + c_{\text{H}_2\text{EN}} \quad (\text{S35})$$

$$c_{\text{NiEN}}^{\text{eff}} = c_{\text{NiEN}} + c_{\text{Ni(EN)}_2} + c_{\text{Ni(EN)}_3} \quad (\text{S36})$$

Eqns. (S31)-(S34) indicate that $k_{\text{a,NiEN}}^{\text{eff}}$ and $k_{\text{d,NiEN}}^{\text{eff}}$ are only constant parameters, independent on the spatial position, whenever the concentration profile of $c_{\text{EN}}^{\text{eff}}$ is homogenous in addition to that of c_{H} . The use of the buffer and the high diffusion coefficient of H ensures the homogeneity of c_{H} . Excess of ligand conditions support a homogeneous profile of $c_{\text{EN}}^{\text{eff}}$. Thus, Equations (S31)-(S34) can be applied to the NiEN system allowing to rewrite the full system as a set of equations formally equivalent to a system with only one reaction, Eqn. (S30).

These effective species allow us to more easily understand the mixing effect, analyzing the concentration profiles, as shown in the main manuscript.

5. Dependence of the lability degree on the ligand concentration in a single ligand system

The dependence of the lability degree on the ligand concentration is especially important for weak complexes, which tend to be labile in excess of ligand conditions and can become almost inert in non-excess of ligand conditions. Lability of strong complexes shows a more moderate dependence on the ligand concentration, since they tend to be already inert or partially labile even in excess of ligand conditions. Figure S4a shows the dependence of the lability degree with the ligand concentration, for different values of the complex stability constant. Figure S4b shows how the relative contribution of the complex to the overall metal accumulation decays with decreasing ligand concentration, while the total metal accumulation rises due to the decreasing ratio of complex and free metal concentrations in bulk solution. The accumulation reaches a maximum value when there is no metal complexed in bulk solution and all the metal is transported to the resin as free metal.

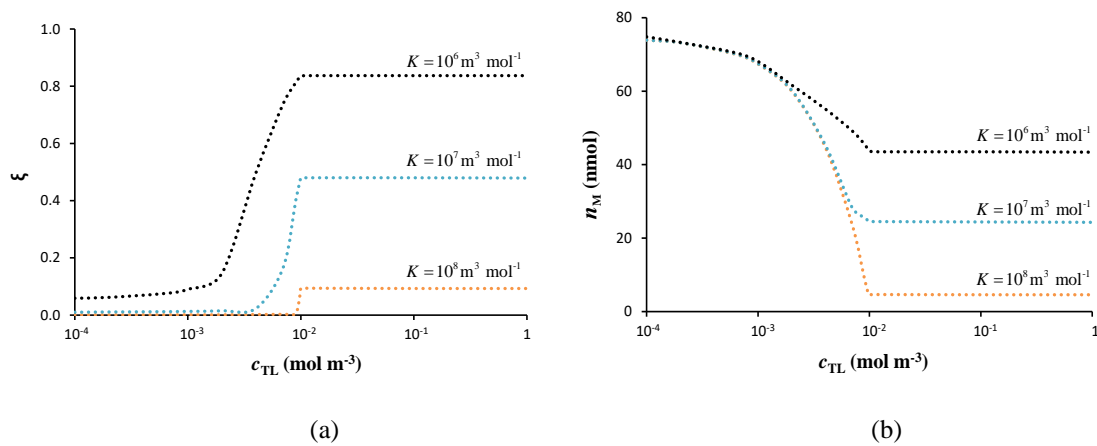


Figure S4. Lability degree of the complex (ξ) and total accumulation of metal (n_M) as functions of c_{TL} in a single ligand system. Results obtained using numerical simulation for different values of stability constant. Parameters used: $c_{TM} = 10^{-2}$ mol m⁻³, $D_M = 6.09 \times 10^{-10}$ m² s⁻¹, $D_L = 4.26 \times 10^{-10}$ m² s⁻¹, $D_{ML} = 4.26 \times 10^{-10}$ m² s⁻¹, $\delta^r = 4 \times 10^{-4}$ m, $\delta^s = 1.1 \times 10^{-3}$ m, $c_{T,R} = 28$ mol m⁻³, $k_a = 10^4$ m³ mol⁻¹ s⁻¹, $t = 10$ h. Perfect-sink conditions between M and the resin sites have been used.

6. Dependence of the metal accumulation on the stoichiometry of MEN complex

Table S9. Percentage of the species formed in the system MEN and moles of metal normalised with bulk concentration accumulated by DGT in a system with EN concentration of 10 mol m^{-3} and $10^{-2} \text{ mol m}^{-3}$ Co, Cu, Cd and Zn and $2.5 \times 10^{-2} \text{ mol m}^{-3}$, $I=6.2 \text{ mol m}^{-3}$ at pH 9.

Component	% of total concentration	Species name	Accumulated nmol/c* (mL)
Ni⁺²	7.805	Ni(EN) ₂	15.34
	92.189	Ni(EN) ₃	
Cd⁺²	3.189	CdEN	15.83
	92.450	Cd(EN) ₂	
	4.347	Cd(EN) ₃	
Co⁺²	45.290	Co(EN) ₂	10.50
	53.492	Co(EN) ₃	
	1.213	CoEN	
Zn⁺²	0.424	ZnEN	16.94
	34.669	Zn(EN) ₂	
	64.897	Zn(EN) ₃	
Cu⁺²	100	Cu(EN) ₂	15.83

7. References

1. Uribe, R.; Puy, J.; Cecilia, J.; Galceran, J. Kinetic Mixture Effects in Diffusion Gradients in Thin Films (DGT). *Phys. Chem. Chem. Phys.* **2013**, *15* (27), 11349-11355.
2. Salvador, J.; Garcés, J. L.; Companys, E.; Cecilia, J.; Galceran, J.; Puy, J.; Town, R. M. Ligand mixture effects in metal complex lability. *J. Phys. Chem. A* **2007**, *111* (20), 4304-4311.
3. Puy, J.; Galceran, J.; Cruz-Gonzalez, S.; David, C. A.; Uribe, R.; Lin, C.; Zhang, H.; Davison, W. Metal accumulation in DGT: Impact of ionic strength and kinetics of dissociation of complexes in the resin domain. *Anal. Chem.* **2014**, *86*, 7740-7748.
4. Sara Cruz-González Availability of metal ions and ZnO nanoparticles in aqueous media. University of Lleida, 2014.
5. Davison, W. *Diffusive Gradients in Thin-Films for Environmental Measurements.*; Cambridge University Press: Cambridge (UK), 2016.
6. Garmo, O. A.; Naqvi, K. R.; Royset, O.; Steinnes, E. Estimation of diffusive boundary layer thickness in studies involving diffusive gradients in thin films (DGT). *Anal. Bioanal. Chem.* **2006**, *386* (7-8), 2233-2237.
7. Warnken, K. W.; Zhang, H.; Davison, W. Accuracy of the diffusive gradients in thin-films technique: Diffusive boundary layer and effective sampling area considerations. *Anal. Chem.* **2006**, *78* (11), 3780-3787.
8. Zhang, H.; Davison, W. Performance characteristics of diffusion gradients in thin films for the insitu measurement of trace metals in aqueous solution. *Anal. Chem.* **1995**, *67* (19), 3391-3400.
9. Mongin, S. Contributions to the study of the availability of metal ions in aquatic systems. PhD thesis. Universitat de Lleida., Jul 2012.
10. Altier, A.; Jimenez-Piedrahita, M.; Rey-Castro, C.; Cecilia, J.; Galceran, J.; Puy, J. Accumulation of Mg to Diffusive Gradients in Thin Films (DGT) Devices: Kinetic and Thermodynamic Effects of the Ionic Strength. *Anal. Chem.* **2016**, *88* (20), 10245-10251.
11. Jimenez-Piedrahita, M.; Altier, A.; Cecilia, J.; Rey-Castro, C.; Galceran, J.; Puy, J. Influence of the settling of the resin beads on Diffusion Gradients in Thin films measurements. *Anal. Chim. Acta* **2015**, *885*, 148-155.
12. Shiva, A. H.; Teasdale, P. R.; Bennett, W. W.; Welsh, D. T. A systematic determination of diffusion coefficients of trace elements in open and restricted diffusive layers used by the diffusive gradients in a thin film technique. *Anal. Chim. Acta* **2015**, *888*, 146-154.

13. Mongin, S.; Uribe, R.; Rey-Castro, C.; Cecilia, J.; Galceran, J.; Puy, J. Limits of the Linear Accumulation Regime of DGT Sensors. *Environ. Sci. Technol.* **2013**, *47*, 10438-10445.